

Citrus sinensis Extract as a Green Inhibitor for the Corrosion of Carbon Steel in Sulphuric Acid Solution

Amira E.Ali¹, Gamila E. Badr¹, Abd El-Aziz S. Fouda^{1,*} 

¹ Chemistry Department, Faculty of Science, Mansoura University, Mansoura-35516, Egypt; asfouda@hotmail.com (A.A.F.); badrgamila@hotmail.com (G.E.B.); ameraali373@yahoo.com (A.E.A.);

* Correspondence: asfouda@hotmail.com;

Scopus Author ID 56231506400

Received: 26.01.2021; Revised: 22.02.2021; Accepted: 25.02.2021; Published: 2.03.2021

Abstract: *Citrus sinensis* extract is considered a good inhibitor to protect the carbon steel in half of molar of sulfuric acid from corrosion, as it was found from the results of chemical methods such as the weight loss (ML) method and also from the results of electrochemical methods such as potentiodynamic polarization (PP), electrochemical impedance spectroscopy (EIS) and electrochemical frequency modulation (EFM). The polarization curves indicated that this extract acts as a mixed kind inhibitor. The adsorption of this extract on the carbon steel surface is of mixed type physisorption and chemisorption, but chemisorption is the most effective one and followed Temkin adsorption isotherm. Several tests have proved a layer that protects carbon steel from corrosion.

Keywords: *Citrus sinensis*; corrosion inhibition; HCl; carbon steel; adsorption.

© 2021 by the authors. This article is an open-access article distributed under the terms and conditions of the Creative Commons Attribution (CC BY) license (<https://creativecommons.org/licenses/by/4.0/>).

1. Introduction

Corrosion is a natural process in which an unstable metal is transformed into a chemically stable form, such as oxide and hydroxide forms, by reacting the mineral chemically or the electrochemical with the surrounding environment [1]. Corrosion is an undesirable phenomenon as it destroys the beneficial properties of the mineral [2]. Metals do not corrode similarly; for example, aluminum metal does not corrode easily like other metals because there is an oxide layer on its surface because it is reactive [3]. Some factors affect corrosion: temperature, impurities such as salts, exposure of minerals to gases such as carbon dioxide, and exposure of minerals to acids in the atmosphere. Most corrosion inhibitors are synthetic chemicals, expensive, and hazardous to the environment. So, the need to use sources of environmentally safe corrosion inhibitors is being required [4, 5]. Green corrosion inhibitors are compounds of plant origin, hence are cheap, biodegradable, and do not contain heavy metals or other n toxic substances. The action of plant extracts on the metal surfaces is the adsorption of the phytochemicals present in the plant onto the metal surface [6, 7], thus preventing the corrosion process from taking place [8-17].

2. Materials and Methods

2.1. CS samples.

The carbon steel composition is shown in Table 1.

Table 1. Chemical composition (weight %) of carbon steel

Material	C	Mn	P	S	Fe
(wt.%)	0.610	0.754	0.013	0.254	Balance

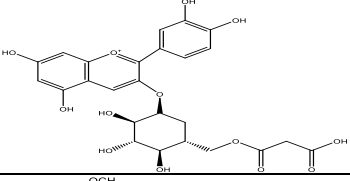
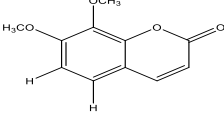
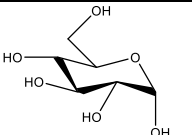
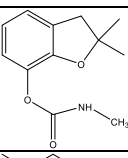
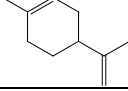
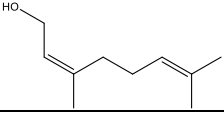
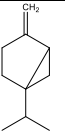
2.2. Plant extract.

Citrus sinensis is used as plant extract in order to protect carbon steel from corrosion.

2.2.1. Chemical composition.

List of some phytochemical constituents isolated from *Citrus sinensis* extract as reported in Table 2:

Table 2. Chemical constituents of *Citrus sinensis* extract.

Name	Structure
Cyanidin 3-(6"-malonylglucoside)	
Limettin	
Glucose	
Carbofuran	
Limonene	
Nerol	
Sabinene	

2.3. Solutions.

Ethyl alcohol, DMF, H₂SO₄, all of the Analar grades, distilled water.

2.4. ML test

The carbon steel metal is divided into pieces of equal length and width and is sanded using sandpaper in degrees of 150, 400, 600, 1000, and 1200, then weighed, and then placed in a half-molar solution of sulfuric acid with and without various doses of the plant extract and then measuring the weight after immersion every half hour for a period of three hours after drying it. Then calculate the percentage of inhibition (%IE) and also surface coverage (θ) by using this equation:

$$\% IE = \theta \times 100 = \left[1 - \frac{W_{inh}}{W_{free}} \right] \times 100 \quad (1)$$

Where W_{nh} is the weight of carbon steel pieces in the existence of extract

W_{free} is the weight of carbon steel pieces in the absence of extract

2.5. Electrochemical methods.

This kind of dissolution is caused between the medium and the metal or the composition, accompanied by the transfer of electrons between two sites on the surface, one of which has a high electron density and another with a low density, or between two points, one of which is of low voltage and the other with a high voltage in the presence of an electrolyte. These methods are the Tafel extrapolation method, linear polarization method, and impedance method. The advantages of these methods are that they take a short time with the highest accuracy [18-21].

The protection efficiency (%IE) and surface coverage (θ) obtained from potentiodynamic polarization (PP) are given by :

$$\% IE = \theta \times 100 = \left[1 - \frac{i_{corr(inh)}}{i_{corr(free)}} \right] \times 100 \quad (2)$$

Where $i_{corr(inh)}$ is the corrosion current density in the existence of the extract.

$i_{corr(free)}$ is the corrosion current density in the absence the extract

2.6. Surface characterization.

2.6.1. Atomic forced microscopy (AFM) analysis.

This method is used to determine the morphology of the carbon steel surface in existence and lack of the extract. Carbon steel parts are dipped in solutions that are prepared in the same way as weight loss in the absence and the highest dose of the extract for a day at room temperature. After this period has passed, these pieces are taken after washing with distilled water and then drying. The surface of carbon steel was analyzed by AFM in contact mode using silicon nitride probe model MLCT manufactured by Bruker, using proscan 1.8 software to control the scan parameters and IP2.1 software.

2.6.2. Fourier Transform Infrared Spectroscopy (FTIR) analysis.

This technique is performed on the extract only and on the layer that protects the carbon steel surface immersed in a half-molar solution of sulfuric acid and the highest dose of the extract for a day.

3. Results and Discussion

3.1. ML method.

The carbon steel strip is divided into 7 equal parts. They are sanded, then weighed. The first piece is placed in a half-molar solution of sulfuric acid, and the rest of the pieces are placed in different doses of the extract from a dose of 50 to 300 ppm for a period of three hours, noting that every half hour, these pieces are taken out after washing with distilled water, then dried and weighed [22-25]. By raising doses, the k_{coo} decreased (\ominus), %IE increased as in Table 3. From Fig. 1 the curves in the presence of various doses of extract lie below that in its absence.

The ML-time curves are approximately lines indicating the absence of oxide film on the carbon steel surface.

Table 3. The rate of corrosion (k_{corr}), surface coverage (Θ), and the efficiency of protection (% IE) at various doses of *Citrus sinensis* extract for carbon steel dissolution after two hours of immersion in 0.5 M H_2SO_4 at 25°C.

Inhibitor	Con.(ppm)	$K_{\text{corr.}}(\text{mg cm}^{-2} \text{min}^{-1})$	Θ	IE%
Blank	0.5 M H_2SO_4	0.0212	----	-----
<i>Citrus sinensis</i>	50	0.01579	0.65	65%
	100	0.006	0.696	69.6%
	150	0.00473	0.777	77.7%
	200	0.0043	0.793	79.3%
	250	0.00384	0.819	81.9%
	300	0.0036	0.836	83.6%

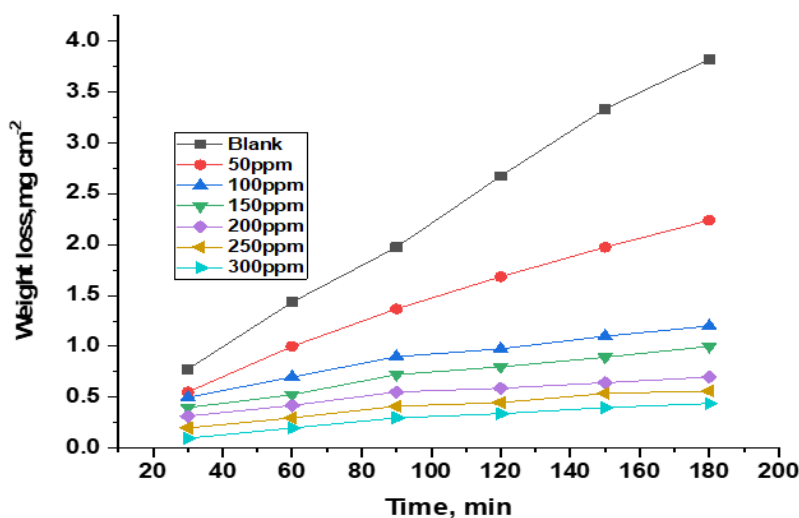


Figure 1. ML- time curves for carbon steel corrosion in 0.5 M H_2SO_4 with and without various concentrations of *Citrus sinensis* extract at 25°C

3.2. Effect of temperature.

Table 4 shows that, by raising the temperature, k_{corr} decreased, (θ) and %IE increased, indicating that the adsorption process is chemisorption [26].

Table 4. The (k_{corr}), (θ), and the (%IE) at various doses of *Citrus sinensis* for C-steel corrosion after immersion of two hours in half of the molar of sulfuric acid.

Conc., ppm	Temp., °C	$k_{\text{corr}}, \text{mg cm}^{-2} \text{min}^{-1}$	θ	%IE
50	25	0.01569	0.65	65%
	30	0.0222	0.677	67.7%
	35	0.0459	0.734	73.4%
	40	0.0481	0.735	73.5%
	45	0.1446	0.794	79.4%
100	25	0.006	0.696	69.6%
	30	0.0082	0.747	74.7%
	35	0.011	0.844	84.4%
	40	0.0164	0.855	85.5%
	45	0.0275	0.879	87.9%
150	25	0.00473	0.777	77.7%
	30	0.0044	0.872	87.2%
	35	0.0067	0.905	90.5%
	40	0.0072	0.937	93.7%
	45	0.01016	0.944	94.4%
200	25	0.0043	0.793	79.3%
	30	0.0042	0.876	87.6%

Conc., ppm	Temp., °C	k_{corr} , $\text{mg cm}^{-2}\text{min}^{-1}$	θ	%IE
250	35	0.0054	0.924	92.4%
	40	0.0061	0.946	94.6%
	45	0.0084	0.954	95.4%
	25	0.00384	0.819	81.9%
	30	0.004	0.877	87.7%
	35	0.0048	0.932	93.2%
	40	0.0059	0.948	94.8%
300	45	0.00787	0.957	95.7%
	25	0.0036	0.836	83.6%
	30	0.0037	0.889	88.9%
	35	0.0047	0.933	93.3%
	40	0.0056	0.951	95.1%
	45	0.0072	0.961	96.1%

3.2.1. Thermodynamic corrosion parameters.

From Arrhenius equation (Fig. 2) Eq. 3, one can calculate E_a^* while from the transition –state equation Eq.4 (Fig. 3), one can determine ΔH^* and ΔS^* for carbon steel in half of molar of sulfuric acid with and without the extract at different temperatures.

$$\text{Log}(k_{\text{corr}}) = \log A - E_a^* / 2.303 RT \quad (3)$$

A log k_{corr} plot versus $1/T$ provided straight lines with slope equivalent- $\Delta E_a^* / 2.303 RT$ from which (ΔE_a^*) values were determined (Fig. 2) by applying the transition-state equation:

$$\log(k_{\text{corr}}/T) = [\log(R/Nh) + ((\Delta S^* / 2.303R) - (\Delta H^* / 2.303RT)] \quad (4)$$

A log plot (k_{corr} / T) versus $1/T$ should give a straight line with a slope of $(-H^* / 2.303R)$ and an intercept of $[\log(R/Nh) + (\Delta S^* / 2.303R)]$ (Fig. 3), respectively, the ΔH^* and ΔS^* values were calculated. From the following table, we found that: 1-The lowest values of E_a^* and ΔH^* in the presence of extract than in its absence indicate that chemical adsorption of extract occurs on the carbon steel surface. 2- Negative ΔS^* values indicate that the adsorbed molecules (products) on carbon steel surface are ordered than in the solution (reactants).

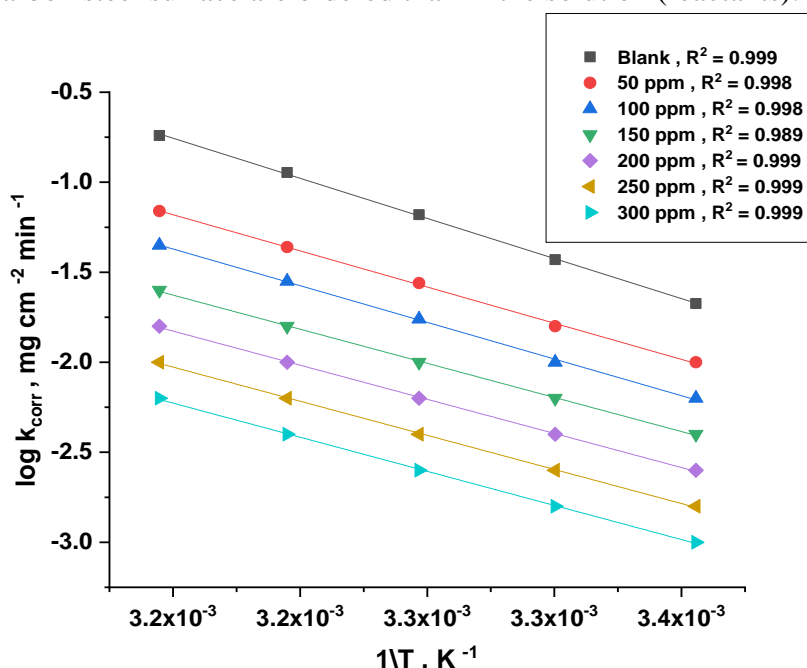


Figure 2. Arrhenius plots for corrosion of carbon steel (k_{corr}) after two hours immersion in 0.5 M H_2SO_4 with and without various doses of *Citrus sinensis*

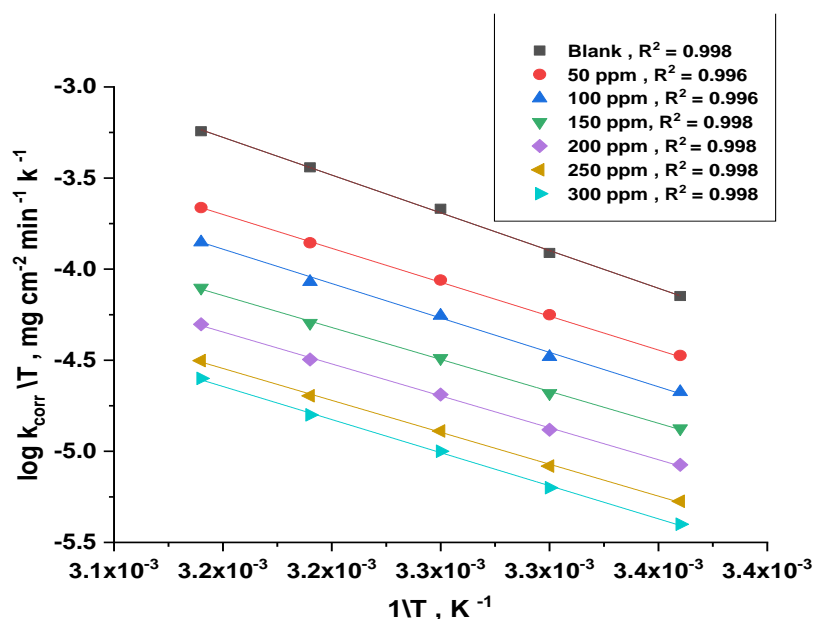


Figure 3. Transition-state log plots (k_{corr}/T) vs. $1/T$ for carbon steel in 0.5 M H_2SO_4 , with and without various doses of *Citrus sinensis* extract.

Table 5. Activation parameters for corrosion with carbon steel in the absence and existence of various extract doses at 0.5 M H_2SO_4

Compound	[inh] ppm	E_a^* kJ mol^{-1}	$^*\Delta H$ kJ mol^{-1}	$-\Delta S^*$ $\text{J mol}^{-1} \text{K}^{-1}$
Blank	0	86.6	80.5	6.8
<i>Citrus Sinensis</i>	50	81.6	75.4	26.8
	100	43.3	40.7	159.3
	150	31.9	29.3	195.9
	200	30.2	27.7	202.4
	250	32.6	30.1	195.9
	300	26.7	24.2	213.9

3.3. Adsorption isotherms

It is found that: This plant extract obeys Temkin adsorption isotherm. Temkin adsorption isotherm is given by the following equation [27]:

$$\Theta_{\text{coverage}} = (2.303a)[\text{Log } K_{\text{ads}} + \text{Log } C] \quad (5)$$

Where Θ : is the surface coverage. K_{ads} : is the adsorption equilibrium constant .a: Heterogeneous factor of CS.

A plot of Θ versus $\log C$ (Fig. 4) should give straight lines with slope equals $(2.303/a)$, and the intercept is $(2.303/a) \text{Log } K_{\text{ads}}$. The $\Delta G^\circ_{\text{ads}}$ can be measured by this equation :

$$K_{\text{ads}} = (1/55.5) \exp(-\Delta G^\circ_{\text{ads}}/RT) \quad (6)$$

Where 55.5: The dose of water at the interface in M.

The adsorption heat ($\Delta H^\circ_{\text{ads}}$) can be calculated according to Van't Hoff's formula, as shown in Fig. 5.

$$\log K_{\text{ads}} = (-\Delta H^\circ_{\text{ads}}/2.303RT) + \text{constant} \quad (7)$$

By plotting $\log K_{\text{ads}}$ against $1/T$ as shown in Fig. 5, the straight line was obtained with a slope equal to $(-\Delta H^\circ_{\text{ads}}/R)$. With the fundamental equation (8) we can calculate $\Delta S^\circ_{\text{ads}}$ at various temperatures.

$$\Delta G^\circ_{\text{ads}} = \Delta H^\circ_{\text{ads}} - T\Delta S^\circ_{\text{ads}} \quad (8)$$

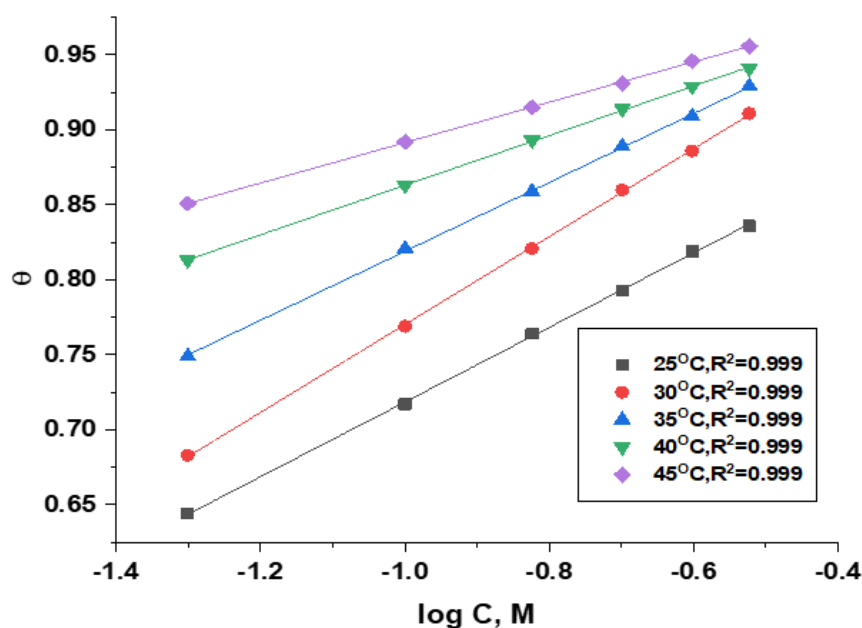


Figure 4. Temkin Adsorption isotherm curves to adsorb *Citrus sinensis* extract on carbon steel at different temperatures in 0.5 M H₂SO₄

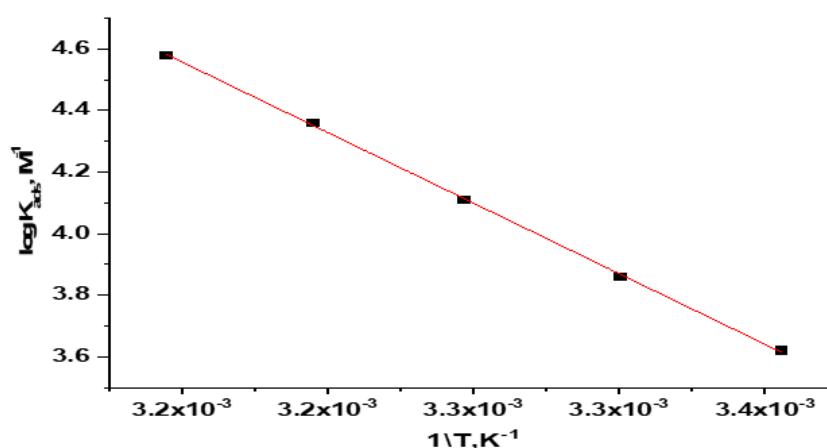


Figure 5. Plots of log K_{ads} vs. 1/ T (Vant Hoff Eq.) for corrosion of carbon steel in 0.5 M H₂SO₄ in the absence and presence of different doses of *Citrus sinensis* extract

Table 6. Thermodynamic parameters of adsorption of *Citrus sinensis* extract at various temperatures on the carbon steel surface in 0.5 M H₂SO₄

Inhibitor	Temperature K	-ΔG ^o _{ads} kJ mol ⁻¹	-ΔH ^o _{ads} kJ mol ⁻¹	-ΔS ^o _{ads} Jmol ⁻¹ K ⁻¹
<i>Citrus sinensis</i>	298	31.2	88.92	396.4
	303	31.9		405.4
	308	34.2		393.4
	313	34.8		401.7
	318	40.7		407.6

From this Table 6, It is found that: The negative values of ΔG^o_{ads} indicate that the adsorption process is spontaneous.

The negative values of (ΔH^o_{ads}) indicate that the adsorption process is exothermic. i.e., the adsorption may be chemical or physical. The value of ΔH^o_{ads} is close to 100 kJ mol⁻¹, so it is a chemical reaction.

3.4. Electrochemical methods.

3.4.1. EIS method.

The advantages of this method are: It doesn't involve a potential scan. It can be applied to low conductivity media. Fig. 6 represents the equivalent circuit used to fit EIS data. In this method, the results have been depicted graphically by Nyquist plots Figs. (7 & 8). As reported before [28], a semicircular impedance spectra in a higher frequency region were depicted in response to the charge transfer, frequency dispersion, mass transfer, and occurrence of a thin protective layer on meta's surface. The charge transfer resistance (R_{ct}) was used to calculate %IE. The double-layer capacity (C_{dl}) is defined as:

$$C_{dl} = Y_o (\omega_{max})^{n-1} \quad (9)$$

Where Y_o is the CPE constant and $\omega = 2\pi f_{max}$ is the angular frequency (rad/s), f is maximum frequency, and n is the parameter deviation for the CPE: $-1 \leq n \leq 1$

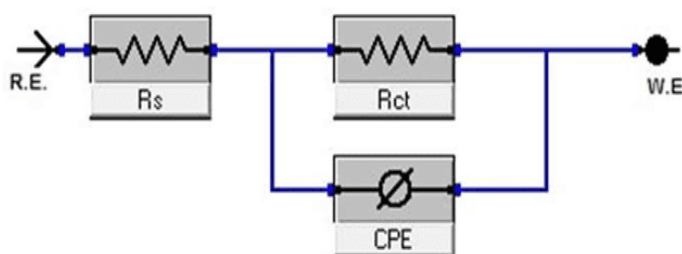


Figure 6. Circuit model used to match experimental EIS

The %IE was calculated as below:

$$\%IE = [1 - R_{ct(inh0)} / R_{ct(free)}] \times 100 \quad (10)$$

The quantitative results obtained from this study are recorded in Table 7. A noticeable increase in %IE is seen in increasing the dose of extract. As reported before [29], by increasing doses of extract, the R_{ct} values increase, and C_{dl} values decrease, which may be ascribed toward the extract's adsorption on the carbon steel surface.

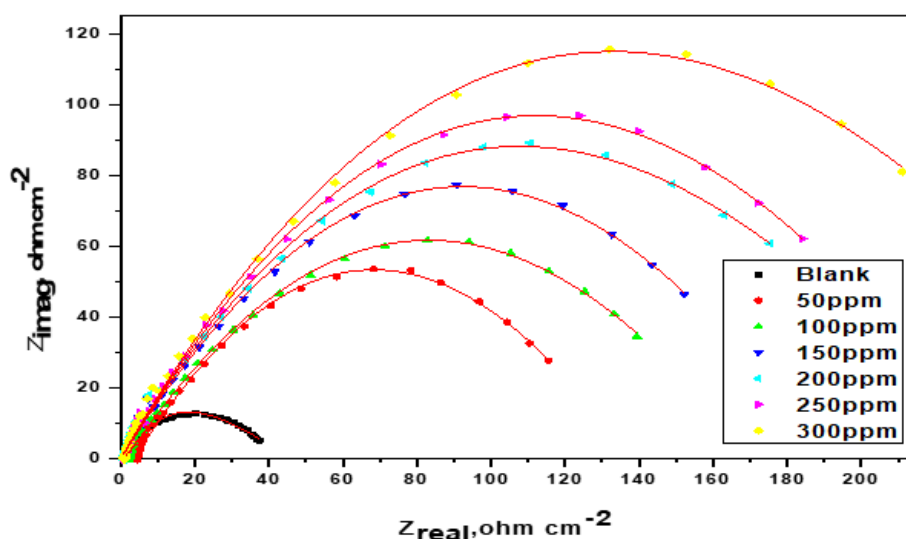


Figure 7. Nyquist plots for carbon steel corrosion in half of the molar of sulfuric acid without and with various *Citrus sinensis* doses at 25°C

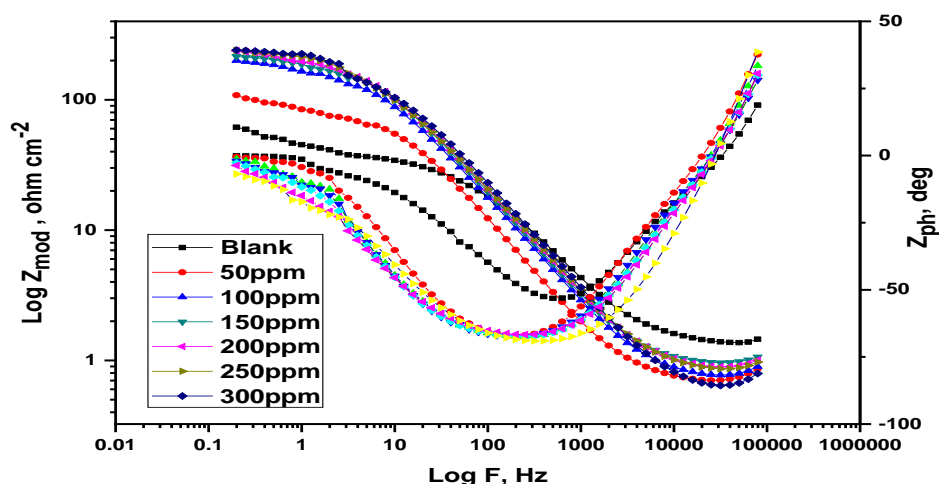


Figure 8. Bode plots for carbon steel corrosion in half of the molar of sulfuric acid with and without various *Citrus sinensis* doses at 25°C.

Table 7. EIS for carbon steel corrosion in half of the molar of sulfuric acid with and without various *Citrus sinensis* doses at 25°C

Conc., ppm	R_{ct} $\Omega \text{ cm}^2$	C_{dl} $\mu\text{F cm}^2$	θ	%IE
Blank	26	214	--	--
50	90.66	168	0.713	71.3
100	93.50	145	0.722	72.2
150	93.76	132	0.723	72.3
200	100.5	111	0.741	74.1
250	125.4	91.9	0.793	79.3
300	131.4	89.9	0.802	80.2

3.4.2. PP technique.

This method determines the rate of metal corrosion quickly. When carbon steel is dipped in the acid solution, which is considered a corrosive medium, oxidation and reduction processes occur on its surface. Tafel is used to describing the mechanism of dissolution of carbon steel in the absence and the existence of the extract [30].

From the following table, we found that:

- 1-From the small changes in the values of E_{corr} (less than ± 85 mV), It shows that the extract is of mixed type [31] (affect on anodic and cathodic reactions) of carbon steel in half of the molar of sulfuric acid as in Table 8.
- 2-The protection efficiency rises with rising the dose of the plant extract, but the density of the corrosion current (i_{corr}) decreases, as in Table 8. This indicates that the extract reduces the dissolution of carbon steel in half of the sulfuric acid.
- 3- Values of β_c , β_a change slightly with rising the dose of the plant extract, meaning that the extract affects the dissolution of the metal and also the hydrogen evolution (i.e., mixed type inhibitor), and the parallel Tafel lines (Fig. 9) indicates that there is no change in the mechanism of the process in presence and absence of the extract [32].

Table 8. Impact of doses of *Citrus sinensis* on (E_{corr}), (i_{corr}), (β_c , β_a), (k_{corr}), (θ) and (% IE) in 0.5 M H_2SO_4 .

Conc. Ppm	i_{corr} $\mu\text{A cm}^2$	$-E_{corr}$ mVvs SCE	β_c mVdec ⁻¹	β_a mVdec ⁻¹	k_{corr} mpy	θ	%IE
0.0	156	549	228.2	71.90	345.4	--	--
50	149	547	169.2	79.70	68.03	0.803	80.3

Conc. Ppm	i_{corr} $\mu A\ cm^{-2}$	$-E_{corr}$ mVvs SCE	β_c mVdec ⁻¹	β_a mVdec ⁻¹	k_{corr} mpy	θ	%IE
100	146	543	124.9	86.40	67.04	0.806	80.6
150	140	541	117.4	54.60	66.92	0.815	81.5
200	123	536	172.5	87	64.01	0.837	83.7
250	102	533	103.4	77.30	56.41	0.865	86.5
300	90	516	157.2	87.60	46.46	0.881	88.1

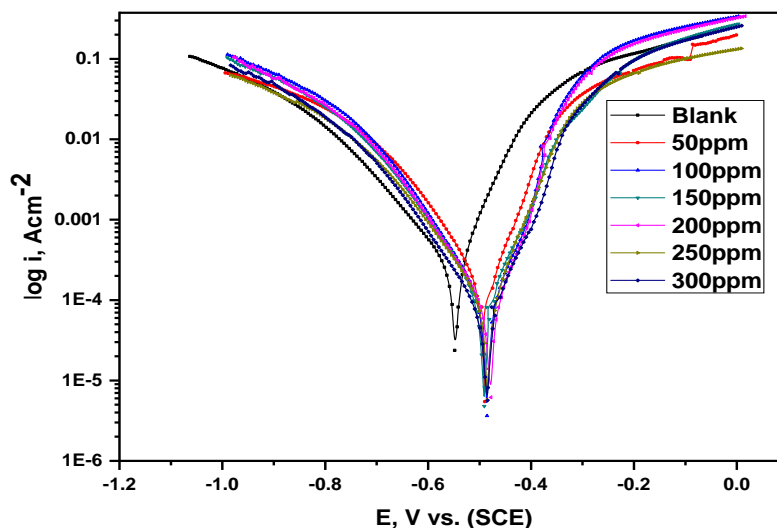


Figure 9. PP curves for the dissolution of carbon steel in half of molar of sulfuric acid with and without various doses of *Citrus sinensis* extract at 25°C.

3.4.3. EFM technique.

This is a non-destructive method for measuring the corrosion of metals in the corrosion medium, and we can also directly calculate the corrosion current. We do not need to know Tafel constants. The corrosion current density (i_{corr}) reduces with raising the plant extract's dose, so the efficiency of the extract increases, as in Table 9. Measured results are of a high quality due to the causality factors' values near their theoretical values (2 & 3) as in Table 9. Fig. 10 shows the intermodulation spectra of carbon steel without and with 300 ppm extract at 25°C.

Table 9. Electrochemical kinetic parameters obtained from EFM technique for carbon steel corrosion in 0.5 M H₂SO₄ without and with various *Citrus sinensis* extract doses at 25°C

Conc., ppm	i_{corr} , $\mu A\ cm^{-2}$	β_a , mV dec ⁻¹	β_c , mV dec ⁻¹	k_{corr} mpy	CF-2	CF-3	θ	%IE
Blank	520	77.2	110.4	122.7	1.854	2.630		
50	240.2	70.4	159.5	103.8	1.869	2.664	0.538	53.8
100	214.1	104.4	119.6	97.81	2.223	2.232	0.588	58.8
150	186	76.4	114.2	85	1.801	3.093	0.642	64.2
200	159.1	89.4	110.7	72.69	1.568	3.124	0.694	69.4
250	135.4	88.2	99.37	67.91	1.686	3.755	0.740	74.0
300	104.9	96.1	121.2	61.88	1.649	3.243	0.800	80.0

3.5. Surface morphology.

3.5.1. AFM technique.

The AFM images of carbon steel in 0.5 M H₂SO₄ and 300 ppm of the extract are presented in Fig. 11 a-c. The average roughness of carbon steel in 0.5 M H₂SO₄ (933.76) is more than the average roughness of carbon steel in 0.5 M H₂SO₄ and the extract's existence (39.767) as in Table 10. This indicates that the surface of the carbon steel has become smooth

due to the formation of a protective layer on its surface from the extract, which leads to the reduction of the corrosion of carbon steel.

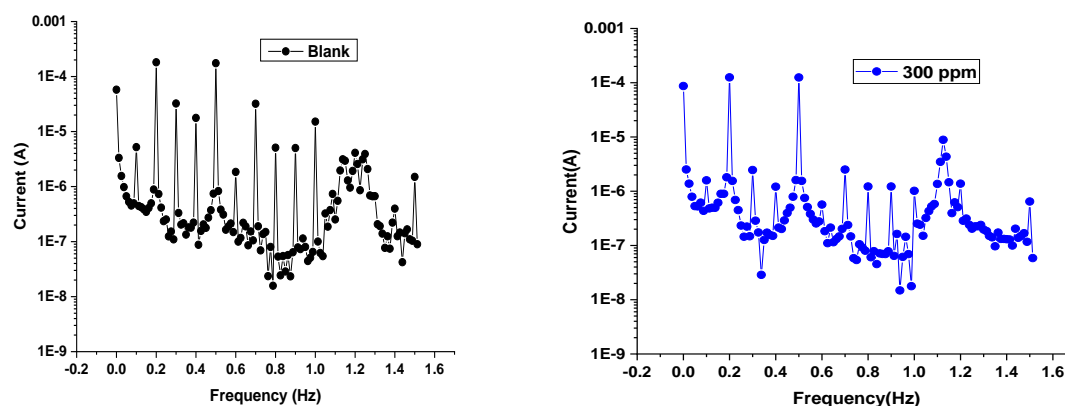


Figure 10. C-steel EFM spectra in 0.5 M H₂SO₄ without and with 300 ppm *Citrus sinensis* extract dose at 25°C.

Table 10. Roughness data obtained for CS by AFM technique [31, 32].

Sample	Average roughness(Sa) [nm]
Polished CS	17.465
CS immersed in 0.5 M H ₂ SO ₄	993.76
CS immersed in 0.5 M H ₂ SO ₄ + 300 ppm of <i>Citrus Sinensis</i>	39.767

3.5.2. FTIR technique.

This technique provides two spectra in the range from 4000 to 400 cm⁻¹. The first spectrometer is the extract alone. While the second one is the carbon steel in the presence of this extract. By comparing the two spectra, we found that there is an interaction between the organic compounds present in the extract and the carbon steel surface forming a layer on the metal surface, and hence, the rate of corrosion decreased.

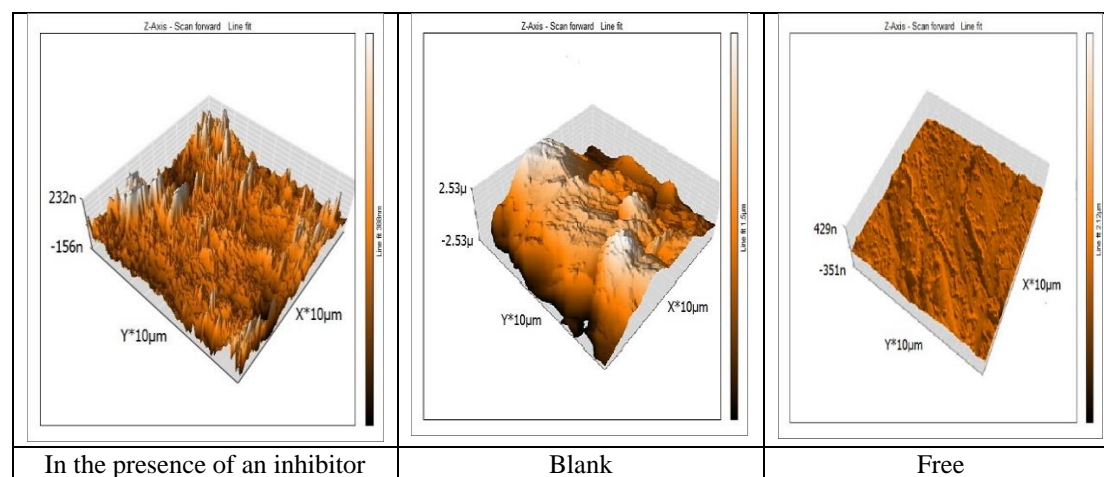


Figure 11. AFM images for carbon steel in (a) inhibited solution of extract (b) blank and (c) free sample.

3.7. Mechanism of inhibition.

The mechanism of inhibition action can be explained based on the mode of adsorption. Adsorption is influenced by the chemical structure of extract, its nature and surface charge, the distribution of charge in the molecule [33].

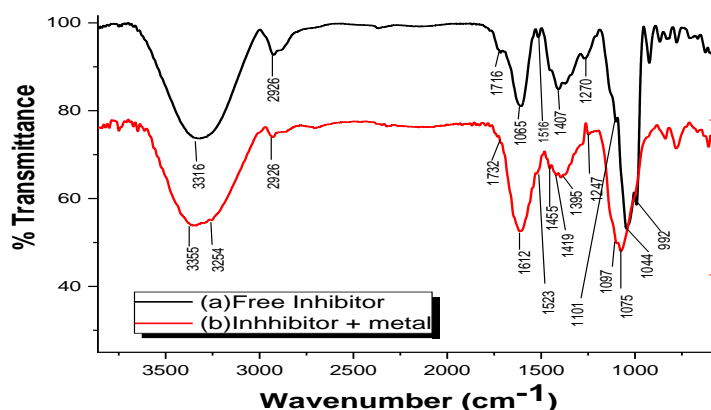


Figure 12. FT – IR spectrum of *Citrus sinensis* before and after adsorption on the carbon steel surface.

Citrus Sinensis extract has electronegative donor atoms N, O, and π -electrons of the aromatic ring. These cause the extract's efficient adsorption on carbon steel surface by sharing lone pair of electrons from these donating atoms to d-orbitals of iron, forming chemical adsorption. Also, the protonated extract molecules tend to adsorb onto the metal surface via electrostatic interaction between the positively charged molecules and the negatively charged metal surface, thus facilitating physical adsorption of the extract molecules, forming a protective film that displaces water molecules from the metal surface and protects it against dissolution.

4. Conclusions

Citrus sinensis extract acts as a good inhibitor for carbon steel corrosion in a 0.5 M H_2SO_4 solution. The inhibition efficiency increased, and the corrosion rate decreased by increasing dose and temperature. The inhibition efficiency of all electrochemical and ML tests was in good agreement. PP measurements demonstrated that the *Citrus sinensis* extract might be a mixed-type inhibitor. EIS measurements showed that the charge transfer resistance increased. The double layer capacitance decreased by increasing *Cirtus sinensis* extract dose and, hence, increasing in % IE. These results can be attributed to the increase in the protective film's thickness formed on the carbon steel surface. The adsorption of *Citrus sinensis* extracts on the carbon steel surface obeyed Temkin adsorption isotherm. The related kinetic and thermodynamic parameters values obtained suggested that both physisorption and chemisorption mechanisms at low temperature while at higher temperature chemisorption mechanism is preferred. The negative sign of $\Delta G^\circ_{\text{ads}}$ values indicated that the adsorption of *Citrus sinensis* extracts molecules on the carbon steel surface spontaneously.

Funding

This research received no external funding.

Acknowledgments

All our gratitude to the anonymous referees for their careful reading of the manuscript and valuable comments helped shape this paper to the present form.

Conflicts of Interest

The authors declare that there is no conflict of interest.

References

1. Liu, T.; Weyers, R. W. Modeling the dynamic corrosion process in chloride contaminated concrete structures. *Cement and Concrete research* **1998**, *28*, 365-379, [https://doi.org/10.1016/S0008-8846\(98\)00259-2](https://doi.org/10.1016/S0008-8846(98)00259-2).
2. Zhang, R.; Castel, A.; François, R. Concrete cover cracking with reinforcement corrosion of RC beam during chloride-induced corrosion process. *Cement and Concrete Research* **2010**, *40*, 415-425, <https://doi.org/10.1016/j.cemconres.2009.09.026>.
3. Wang, Y.; Wei, M.; Gao, J.; Hu, J.; Zhang, Y. Corrosion process of pure magnesium in simulated body fluid. *Materials letters* **2008**, *62*, 2181-2184, <https://doi.org/10.1016/j.matlet.2007.11.045>.
4. Benarioua, M.; Mihi, A.; Bouzeghaia, N.; Naoun, M. Mild steel corrosion inhibition by Parsley (*Petroselinum Sativum*) extract in acidic media. *Egyptian Journal of Petroleum* **2019**, *28*, 155-159, <https://doi.org/10.1016/j.ejpe.2019.01.001>.
5. Elabbasy, H.M.; Zidan, S.M.; El-Aziz, A.F.S. Inhibitive behavior of Ambrosia Maritima extract as an eco-friendly corrosion inhibitor for carbon steel in 1M HCl. *Zaštita materijala* **2019**, *60*, 129-146, <https://doi.org/10.5937/zasmat1902129E>.
6. Elabbasy, H.M.; Fouda, A.S. Olive leaf as green corrosion inhibitor for C-steel in Sulfamic acid solution. *Green Chemistry Letters and Reviews* **2019**, *12*, 332-342, <https://doi.org/10.1080/17518253.2019.1646812>.
7. Fouda, A.E.-A.S.; Eissa, M. Adenium obesum Extract as a Safe Corrosion Inhibitor for C-Steel in NaCl Solutions: Investigation of Biological Effects. *Journal of Bio- and Tribo-Corrosion* **2020**, *6*, 1-11, <https://doi.org/10.1007/s40735-020-00394-3>.
8. Almazrie, K.; Falah, A.; Massri, A.; Kellawi, H. Electrochemical Impedance Spectroscopy (EIS) and Study of Iron Corrosion Inhibition by Turmeric Roots Extract (TRE) in Hydrochloric Acid Solution. *Egyptian Journal of Chemistry* **2019**, *62*, 501-512, <https://dx.doi.org/10.21608/ejchem.2018.5295.1476>.
9. Addi, B.; Addi, A.; Shaban, A.; Habib, E.; Ait Addi, E.H.; Hamdani, M. Tin corrosion inhibition by molybdate ions in 0.2 M maleic acid solution: Electrochemical and surface analytical study. *Mediterranean Journal of Chemistry* **2020**, *10*, 465-476, <http://dx.doi.org/10.13171/mjc10502005141394aa>.
10. Mukemre, M.; Konczak, I.; Uzun, Y.; Dalar, A. Phytochemical profile and biological activities of Anatolian Plantain (*Plantago anatolica*). *Food Bioscience* **2020**, *36*, <https://doi.org/10.1016/j.fbio.2020.100658>.
11. Genc, Y.; Dereli, F.T.G.; Saracoglu, I.; Akkol, E.K. The inhibitory effects of isolated constituents from *Plantago major* subsp. *major* L. on collagenase, elastase and hyaluronidase enzymes: Potential wound healer. *Saudi Pharmaceutical Journal* **2020**, *28*, 101-106, <https://doi.org/10.1016/j.jsps.2019.11.011>.
12. Fernandes, C.M.; Ferreira Fagundes, T.d.S.; Escarpini dos Santos, N.; Shewry de M. Rocha, T.; Garrett, R.; Borges, R.M.; Muricy, G.; Valverde, A.L.; Ponzio, E.A. Ircinia strobilina crude extract as corrosion inhibitor for mild steel in acid medium. *Electrochimica Acta* **2019**, *312*, 137-148, <https://doi.org/10.1016/j.electacta.2019.04.148>.
13. Saraswat, V.; Yadav, M. Computational and electrochemical analysis on quinoxalines as corrosion inhibitors for mild steel in acidic medium. *Journal of Molecular Liquids* **2020**, *297*, <https://doi.org/10.1016/j.molliq.2019.111883>.
14. Ouakki, M.; Galai, M.; Rbaa, M.; Abousalem, A.S.; Lakhri, B.; Touhami, M.E.; Cherkaoui, M. Electrochemical, thermodynamic and theoretical studies of some imidazole derivatives compounds as acid corrosion inhibitors for mild steel. *Journal of Molecular Liquids* **2020**, *319*, <https://doi.org/10.1016/j.molliq.2020.114063>.
15. Al-Nami, S. Corrosion Inhibition Effect and Adsorption Activities of methanolic myrrh extract for Cu in 2 M HNO₃. *International Journal of Electrochemical Science* **2020**, *15*, 1187-1205, <https://doi.org/10.20964/2020.02.23>.
16. Zhang, S.; Hou, L.; Du, H.; Wei, H.; Liu, B.; Wei, Y. A study on the interaction between chloride ions and CO₂ towards carbon steel corrosion. *Corrosion Science* **2020**, *167*, <https://doi.org/10.1016/j.corsci.2020.108531>.
17. El-Aziz, E.S.F.A.; Mahmoud, R.S.; Ibrahim, H.; Ezzat, A.R. Expired nizatidine drug as eco-friendly corrosion Inhibitor for alpha-brass alloy in aqueous solutions. *Zaštita materijala* **2020**, *61*, 192-209.
18. Qiang, L.X.; Shijin, C.; Jiahong, H. Papaya leaves extract as a novel eco-friendly corrosion inhibitor for Cu in H₂SO₄ medium. *Journal of Colloid and Interface Science* **2020**, *582*, 918-931, <https://doi.org/10.1016/j.jcis.2020.08.093>.
19. Xiao, L.; Jianxin, P.; Jianren, Z.; Yafei, M.; Cai, C.S. Comparative assessment of mechanical properties of HPS between electrochemical corrosion and spray corrosion. *Construction and Building Materials* **2020**, *237*, <https://doi.org/10.1016/j.conbuildmat.2019.117735>.
20. Aslam, J.; Aslam, R.; Lone, I.H.; Radwan, N.R.; Mobin, M.; Aslam, A.; Alzulaibani, A.A. Inhibitory effect of 2-Nitroacridone on corrosion of low carbon steel in 1 M HCl solution: An experimental and theoretical

- approach. *Journal of Materials Research and Technology* **2020**, *9*, 4061-4075, <https://doi.org/10.1016/j.jmrt.2020.02.033>.
21. Qiu, J.; Li, Y.; Xu, Y.; Wu, A.; Macdonald, D.D. Effect of temperature on corrosion of carbon steel in simulated concrete pore solution under anoxic conditions. *Corros. Sci.* **2020**, *175*, <https://doi.org/10.1016/j.corsci.2020.108886>.
 22. Motawea, M. M.; El-Hossiany, A.; Fouda, A.S. Corrosion Control of Copper in Nitric Acid Solution using Chenopodium Extract. *Int. J. Electrochem. Sci.* **2019**, *14*, 1372–1387, <https://doi.org/10.20964/2019.02.29>.
 23. Zhu, H.; Huo, Y.; Wang, W.; He, X.; Fang, S.; Zhang, Y. Quantum chemical calculation of reaction characteristics of hydroxyl at different positions during coal spontaneous combustion. *Process Safety and Environmental Protection* **2021**, *148*, 624-635, <https://doi.org/10.1016/j.psep.2020.11.041>.
 24. Fouda, A.S.; Abd El-Maksoud, S.A.; El-Hossiany, A.; Ibrahim, A. Corrosion Protection of Stainless Steel 201 in Acidic Media using Novel Hydrazine Derivatives as Corrosion Inhibitors. *Int. J. Electrochem. Sci.* **2019**, *14*, 2187-2207, <https://doi.org/10.20964/2019.03.15>.
 25. Melchers, R.E. Effect of temperature on the marine immersion corrosion of carbon steels. *Corrosion*, **2002**, *58*, 768-782, <https://doi.org/10.5006/1.3277660>.
 26. Fouda, A.S.; El-Gharkawy, E.; Ramadan, H.; El-Hossiany, A. Corrosion Resistance of Mild Steel in Hydrochloric Acid Solutions by Clinopodium acinos as a Green Inhibitor, *Biointerface Research in Applied Chemistry* **2021**, *11*, 9786–9803, <https://doi.org/10.33263/BRIAC112.97869803>.
 27. Fouda, A.S.; Abdel Azeem, M.; Mohamed, S.A.; El-Hossiany, A.; El-Desouky, E. Corrosion Inhibition and Adsorption Behavior of Nerium Oleander Extract on Carbon Steel in Hydrochloric Acid Solution. *Int. J. Electrochem. Sci.* **2019**, *14*, 3932–3948, <https://doi.org/10.20964/2019.04.44>.
 28. Bashir, S.; Singh, G.; Kumar, A. Shatavari (*Asparagus Racemosus*) as green corrosion inhibitor of aluminium in acidic medium, *J Mater Environ Sci.*; **2017**, *8*, 4284–4291, <https://doi.org/10.26872/jmes.2017.8.12.451>.
 29. Fouda, A.S.; Rashwan, S.; El-Hossiany, A.; El-Morsy, F.E. Corrosion Inhibition of Zinc in Hydrochloric Acid Solution using some organic compounds as Eco-friendly Inhibitors. *Journal of Chemical, Biological and Physical Sciences* **2019**, *9*, 001-024, <https://doi.org/10.24214/jcbps.A.9.1.00124>.
 30. Zhu, H.; Huo, Y.; Wang, W.; He, X.; Fang, S.; Zhang, Y. Quantum chemical calculation of reaction characteristics of hydroxyl at different positions during coal spontaneous combustion. *Process Safety and Environmental Protection* **2021**, *148*, 624-635, <https://doi.org/10.1016/j.psep.2020.11.041>.
 31. Fouda, A.S.; Eissa, M.; El-Hossiany, A. Ciprofloxacin as Eco-Friendly Corrosion Inhibitor for Carbon Steel in Hydrochloric Acid Solution. *Int. J. Electrochem. Sci.* **2018**, *13*, 11096–11112, <https://doi.org/10.20964/2018.11.86>.
 32. Fouda, A.S.; Abd El-Maksoud, S.A.; El-Hossiany, A.; Ibrahim, A. Effectiveness of Some Organic Compounds as Corrosion Inhibitors for Stainless Steel 201 in 1M HCl: Experimental and Theoretical Studies. *Int. J. Electrochem. Sci.* **2018**, *13*, 9826–9846, <https://doi.org/10.20964/2018.10.36>.
 33. Eid, A.M.; Shaaban, S.; Shalabi, K. Tetrazole-based organoselenium bi-functionalized corrosion inhibitors during oil well acidizing: Experimental, computational studies, and SRB bioassay. *Journal of Molecular Liquids* **2020**, *298*, <https://doi.org/10.1016/j.molliq.2019.111980>.